Journal of Material Cycles and Waste Management (2023) 25:128–143
https://doi.org/10.1007/s10163-022-01519-1

ORIGINAL ARTICLE

Ferronickel slag as free-draining rockfill dike material: a novel waste solution for mining regions

João Paulo R. Costa[1] · Guilherme J. C. Gomes[1,2] · Gilberto Fernandes[1] · Dario M. Magarinos[3] · Alberto Fonseca[2] · Patrício J. M. Pires[4]

Received: 3 April 2022 / Accepted: 27 September 2022 / Published online: 5 October 2022

Abstract

Mining sites are vulnerable to erosion and siltation of rivers. While the construction of rockfill dikes can mitigate siltation, existing rockfill dikes are typically constructed with natural aggregates, whose mining, beneficiation, and transportation entail additional adverse impacts. In this paper, ferronickel slag (FNS) was investigated as a free-draining rockfill dike material to be used in nearby mining sites. A series of laboratory tests, including physical, environmental, durability, chemical and mineralogical analyzes, was executed to evaluate the engineering characteristics of this byproduct and its potential use in dikes. Results demonstrate that FNS is non-uniform with relatively low Los Angeles abrasion. Leaching and dissolution tests have not shown harm to the environment since the average concentrations of chemical elements existing in FNS were below the standard requirements. Accelerated weathering cycling tests with ethylene glycol further highlighted that the byproduct does not suffer premature disaggregation in the presence of water, thereby revealing that the material can be employed adequately under saturated condition. Findings suggest that the use of FNS in rockfill dikes represents a technically and environmentally feasible solution, while reducing the use of natural aggregates, avoiding the formation of stockpiles, preventing siltation in downstream fluvial networks and other adverse impacts.

Keywords Ferronickel slag (FNS) · Rockfill material · Industrial ecology · Sediment dike · Environmentally friendly materials

✉ Guilherme J. C. Gomes
guilhermejcg@ufop.edu.br

João Paulo R. Costa
jpreng@gmail.com

Gilberto Fernandes
gilberto@ufop.edu.br

Dario M. Magarinos
dario.magarinos@aluno.ufop.edu.br

Alberto Fonseca
alberto@ufop.edu.br

Patrício J. M. Pires
patricio.pires@gmail.com

[1] Graduate Program in Geotechnics, Federal University of Ouro Preto, Ouro Preto, Minas Gerais, Brazil

[2] Department of Environmental Engineering, Federal University of Ouro Preto, Ouro Preto, Minas Gerais, Brazil

[3] School of Mines, Federal University of Ouro Preto, Ouro Preto, Minas Gerais, Brazil

[4] Department of Civil Engineering, Federal University of Espírito Santo, Vitória, Espírito Santo, Brazil

Introduction

While mining and metallurgical companies have long been envisioning a sustainable industry [1], numerous challenges remain to the realization of this scenario [2]. For example, the mineral sector generates large volumes of waste for which there are no easy management solutions. Among these is the ferronickel slag (FNS), a waste generated during the smelting of nickel ores in electric arc furnaces [3], which may contain large amounts of silica, magnesium, and iron oxides, in addition to aluminum and calcium oxides [4–7]. It has been estimated that to produce one ton of nickel alloy, 12–14 tons of FNS are generated [8]. Unfortunately, the largest portion of the FNS produced remains stockpiled [6, 9–11], since several factors restrict the reuse of this byproduct. For instance, the high content of MgO, which can cause poor stability (i.e., excessive expansion) when in contact with water [12, 13], is a remarkable challenge that inhibits the usage of FNS as a construction material [14]. Yet, as this byproduct has also demonstrated excellent engineering

properties, there are opportunities to expand applications of FNS as a building material, enabling its recycling and minimizing the consumption of natural resources [7, 15].

The growth of nickel mining [16] has been accompanied by the generation of FNS and its stockpiles at metallurgical sites [13]: a fact that explains the increasing number of academic studies on the engineering properties of eco-friendly FNS-based materials and applications. This includes laboratory experiments to produce concrete [15, 17], mortar [8], hot mix asphalt [18], ceramic tiles [19], fertilizer [20], geopolymer [9], glass fiber [21], glass–ceramics [22], and as a source of magnesium metal and ferroalloy production [23]. This body of work has found that replacement of natural aggregates by FNS enabled the development of high-strength structural concrete (e.g., [24, 25]). Furthermore, soundness and strength development of FNS-based cement pastes and mortars were similar as those of commonly adopted supplementary cementitious materials [26]. From an environmental perspective, the leaching of heavy metals from concrete samples containing FNS was much below the Dutch regulatory limits [24]. Despite the non-hazardous characteristic of FNS [11], some jurisdictions still treat this byproduct as a hazardous waste [27], which makes the management of this material particularly challenging. Altogether, these previous studies have focused primarily on understanding the engineering properties of FNS as aggregate of composite materials rather than exploring its properties as raw materials.

While there have been studies showing the feasibility of incorporating FNS in construction materials (e.g., cement and concrete) [24], such solutions may not necessarily be cost-effective or environmentally friendly, depending on the amount (and location) of these wastes [28]. Through an industrial ecology lens [29], FNS should find an ideal application close to its generation source, thus minimizing the need for transportation and its adverse impacts on the environment. Accordingly, uses of FNS that preserve the engineering properties of natural aggregates and are applied close to mining and steelmaking facilities should be preferred from a sustainability standpoint. Therefore, a natural question is whether this byproduct can be used to mitigate environmental impacts in mining regions. This paper addresses this research gap.

It stands out, for example, that open pit mining sites in erosive landscapes, including those in nickel mining regions, have long tried to control sediments produced by water and wind erosion [30–32]. Zapico et al. [33] have recently argued that sediments produced by water erosion are still one of the most challenging environmental impacts in the industry. To address this problem, mining companies have been adopting various solutions, such as avoiding the exposure of sediment-generating materials to wind or water, diverting runoff from undisturbed areas around mined areas, protecting storm-water drains, ditches, and stream channels against erosion, re-vegetating disturbed areas, and using temporary and permanent installations such as dikes, berms, gabions, and other sediment barriers. Rockfill dikes, also known as rock filter dikes or embankments, have been increasingly used in mining sites due to their effectiveness and flexibility [34], as these structures often employ on site or nearby (quarry) materials [35]. Yet, this is not necessarily valid in all geographical contexts, since the distance between quarries and the demand points are getting progressively longer [36].

Rockfill materials should have substantial strength, specific gravity, and permeability [37]. Literature findings suggest that slag raw materials meet such requirements [38]. For example, the specific gravity of FNS is 10–25% higher than natural aggregates, enabling its explicit use as raw material in structures such as gravity retaining walls, cable anchors, wave-dissipating blocks and rockfill dikes [7]. Rockfill dike is a coarse-grained, free-draining hydraulic structure, frequently composed of quarry or riverbed rocks [34, 39]. These hydraulic structures are used to contain silts at the outlet of watersheds during a rain event. According to Siddiqua et al. [40], most existing rockfill dikes are conceived as flow-through dikes by taking advantage of the porous nature of the rockfill material. By retaining silts in a filter, these structures allow sediment-free water to percolate through the dike, thereby reducing adverse environmental effects in downstream rivers.

Whereas much progress has been made on the characterization of FNS for the development of environmentally friendly composite materials, surprisingly, to the best of the authors' knowledge, no attention has been given to the investigation of this byproduct as a free-draining rockfill dike to retain sediments in mining regions. Careful examination of the behavior of rockfill materials is essential to the realistic evaluation and design of rockfill structures [41]. This requires an analysis of specific properties of the FNS raw material, including grain-size distribution, durability, leaching characteristics and weathering resistance. Being aware of this fact, this study set out to investigate the use of FNS as a free-draining rockfill dike material in one of Brazil's largest iron and nickel producing sites, where this metallurgical waste has been accumulated in large stockpiles. More specifically, this study carried out a series of laboratory tests, including physical, environmental, mechanical, chemical and mineralogical analyzes, to evaluate the engineering characteristics of this byproduct and its potential use in free-draining rockfill dikes.

Materials and methods

Materials

FNS, obtained from a Brazilian multinational mining-metallurgical company, located in the north of the country, was

used as raw material in this study. Figure 1 provides the geographic overview of the study area, sampling of stockpiled material and the general appearance of the byproduct. To date, the volume of FNS in the stockpile is approximately 2 million cubic meters, occupying a relatively large area of 140.12 ha. The sampling locations are depicted with blue colored areas, representing investigations at Locations 1 (light blue), 2 (medium blue) and 3 (sky blue). These sampling locations differ in their nickel content and deposition period. As indicated in Fig. 1, the byproduct samples were collected at 12 points, equally distributed in the three locations using a backhoe, down to a depth of 10–70 cm. The byproduct samples were packed in 30 kg plastic bags, sealed, and further investigated in the laboratory.

The main physical properties of the byproduct FNS, obtained from the company database according to the Brazilian standard ABNT NBR 5564 [42], are listed in Table 1, including specific gravity (SG), unconfined compressive strength (UCS), maximum particle dimension (D_{max}), apparent porosity (P), and water absorption (WA). The sample used in the UCS test was obtained after extracting a specimen from an undisturbed block.

The expansion of the mining activities in the region is generating large volumes of sediments. These are generated in ore storage yards and waste rock piles, and from a large portion of the mining area, corresponding to a basin of 413 ha. Silt traps have been constructed (Fig. 2a) within the mining area at several places to decrease the silt loads reaching the outlet. These silt traps are small settling reservoirs constructed by excavation. Their main function is to capture sediment-laden runoff from the mining site for enough time, allowing most of the sediment to settle out. Unfortunately, in the study area, these devices are not enough to reduce the adverse effects of runoff discharge from the mining site to downstream rivers, which can be achieved with the construction of free-draining rockfill dikes. Clayey sediment samples were collected at five different sediment traps of the mining site (Fig. 2b). The sediment samples were packed in 30 kg plastic bags and sealed for further granulometric analysis in the laboratory. The sedimentation method [43] was adopted here to establish the particle size distribution of the sediment that is finer than the 0.074 mm sieve (or sieve #200).

Table 1 Basic physical and water absorption properties of FNS

SG (–)	UCS (MPa)	D_{max}(mm)	P(%)	WA (%)
3.3	139	63	3.7	1.2

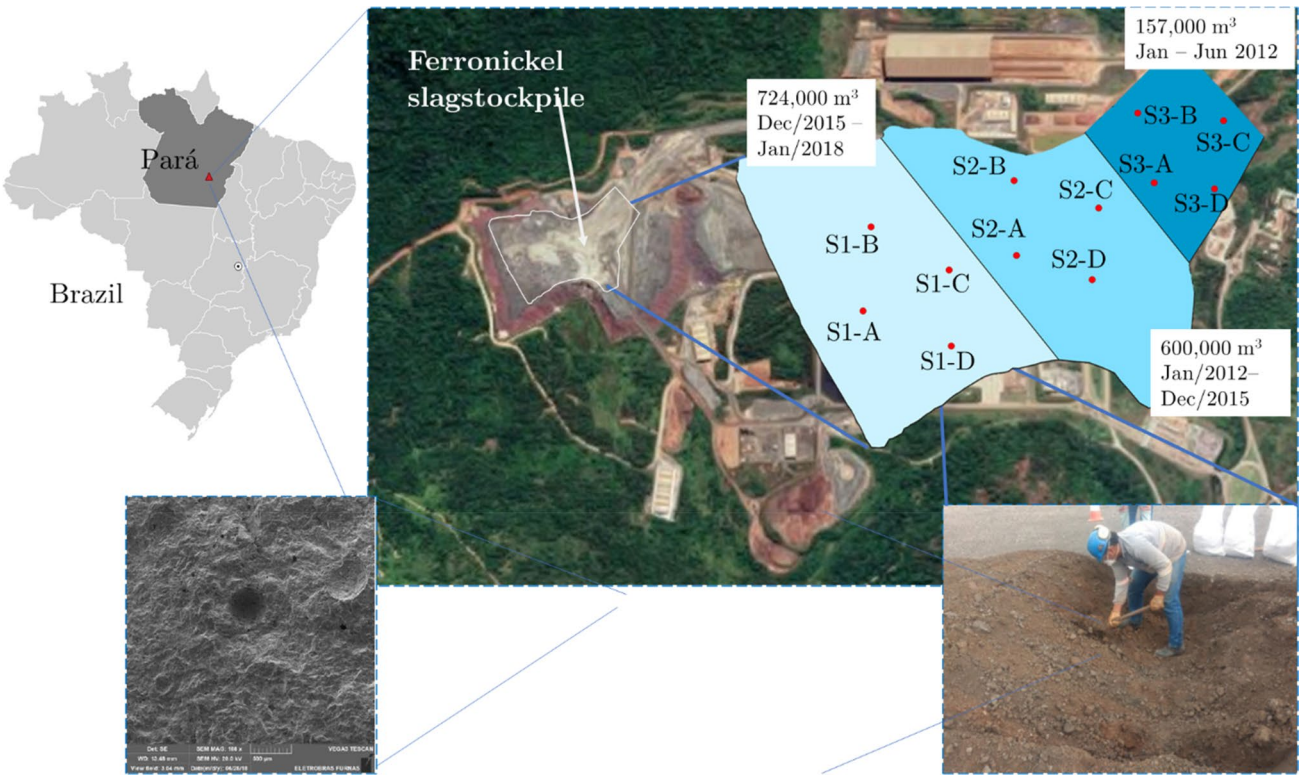

Fig. 1 Overview of the study area in northern Brazil, sampling and appearance of the ferronickel byproduct investigated. The sampling locations are indicated with red dots. The different blue colors of the stockpile represent byproducts with distinct nickel content and deposition period

(a)

(b)

Fig. 2 Appearance of the silt generated from various mine operations: **a** overview of one of the sediment traps and **b** silt (sediment) sampling

Experimental methodology

A series of performance tests were executed on FNS to evaluate its feasibility as a rockfill dike material. In the absence of a specific standard for the use of this material in the construction of rockfill dikes, tests deemed essential for the characterization of the byproduct were carried out. Table 2 lists the series of laboratory experiments performed, including physical, environmental, durability, chemical and mineralogical tests, which supplied data for the dike design. In addition, engineering properties involved in the utilization of natural aggregates as rockfill (dam) materials were evaluated for comparative analysis. The next subsections detail the different experiments listed in Table 2.

Test methods

Physical characterization

The particle size distribution of FNS materials was performed by sieve analyzes according to the Brazilian standard NBR 7181 [43]. This is the standard reference for particle size analysis of granular materials in Brazil. For the fraction below 0.075 mm, sedimentation analysis was performed. The particle size distribution test results were further used to define geometric parameters based on the grading curve, that is, the maximum particle dimension (D_{max}), the fineness modulus (F_m), the coefficient of uniformity (C_u) and the coefficient of curvature (C_c). F_m is obtained by adding the total percentage of the aggregate sample retained in a standard series of sieves and dividing the sum by 100. The standard sieves are: 37.5, 4.75, 1.20, 0.60, 0.30 and 0.15 mm. The higher the F_m, the coarser the aggregate is. C_u is defined as D_{60}/D_{10}, where D_{60} and D_{10} are the diameters corresponding to 60% and 10% finer, respectively. C_c is defined as ${D_{30}}^2/(D_{60} \times D_{10})$, where D_{30} is the diameter corresponding to 30% finer.

Los Angeles abrasion (LAA) tests were executed according to the Brazilian standard NBR-NM 51 [44], which is similar to the ASTM C 131/89 standard. This test is recommended for the characterization of aggregates as it simulates friction between particles and the breakage of FNS samples. The tests were carried out using byproduct sizes between 9.5 and 19 mm. The byproducts (5 kg) were dried at 107 °C for 24 h and then cooled to room temperature. After that, the FNS samples were placed in a steel drum with eleven steel spheres (approximately 4584 g). The drum was rotated for 500 revolutions at a rate of 30–33 revolutions per minute. After the 500 revolutions were finished, the byproduct samples were separated from the steel spheres and then the

Table 2 Summary of laboratory experimental tests performed, including physical, environmental, durability, chemical and mineralogical tests

Characterization	Experiments	Standard references
Physical	Particle size	NBR 7181 [43]
	Los Angeles abrasion	NBR-NM 51 [44]
Environmental	Leaching	NBR 10005 [45]
	Solubilization	NBR 10006 [46]
Durability	Cycling	NBR 12697 [47]
Chemical and mineralogical	X-ray diffraction	
	Scanning electron microscopy	
	X-ray fluorescence	

crushed byproduct particles were sieved through a 1.7 mm sieve. The quantity of FNS passing through the sieve, indicated as a percentage of the original mass, is defined as the LA abrasion resistance or percentage loss. 24 FNS samples were collected from the three sampling regions in Fig. 1 (8 samples for each region or 2 samples for each sampling point). The mean results of the LA tests for the three sampling regions were summarized in bar plots.

Environmental characterization

To estimate the level of contamination of potentially toxic elements, environmental characterization including leaching and solubilization (dissolution) experiments were conducted on byproduct samples. The leaching test followed the protocol established by the Brazilian standard NBR 10005 [45], which is equivalent to the toxicity characteristic leaching procedure (TCLP), detailed in the EPA method 1311 [48]. Chemical elements were determined by Inductively Coupled Plasma Optical Emission Spectroscopy (ICP-OES, model Optima 7300DV, Perkin-Elmer, USA). Solubilization tests must be executed on non-hazardous byproducts to verify if the material is inert or non-inert, that is, whether or not the concentrations of the chemical elements, after solubilization, are below than the recommended requirements for drinking water quality, respectively. According to the Brazilian standard NBR 10006 [46], 250 g of crushed byproduct sample were dissolved in 1000 mL of ultra-pure water. The mixture then remained at rest and was manually stirred from time to time for a period of 7 days. After this period, the sample was filtered, and the filtered material was further examined by spectrophotometric analysis. Based on the Brazilian standard NBR 10004 [49], waste materials can be classified in three different categories: class I (hazardous), class II A (non-hazardous, non-inert) and class II B (non-hazardous, inert). The last class represents the best possible classification for a byproduct.

Material durability

Following the procedures outlined in the Brazilian standard NBR 12697 [47], cycling tests were executed to evaluate the behavior of the byproduct through accelerated weathering cycling with ethylene glycol. This test method can detect the presence of clay minerals in byproduct particles. The presence of such clay minerals is associated with material (generally rock) degradation during wetting and drying cycles [50]. Ethylene glycol penetrates into the reticulated structure of expansive minerals, such as smectite and vermiculite, causing expansion and fractures in the byproduct particles that contain these minerals [51]. As a consequence, this experiment can be used to analyze the durability of FNS.

The cycling tests involved 3-kg samples of byproduct with fractions ranging between 75 and 19 mm (i.e., material passing through a 75-mm sieve and retained on a 19-mm sieve). The weighed samples were then washed in water to remove dust. The washed samples were dried back in an oven to a constant mass before photographed (Fig. 3). Next, the samples were soaked for 16 days in ethylene glycol, and then they were carefully cleaned and dried back in the oven. Finally, the quantitative metric of this mechanical test is the change in mass of the byproduct between the last weighing day (final cycle) in relation to the initial weight (initial cycle). 12 FNS samples were collected from the three sampling regions in Fig. 1 (4 samples for each region or 1 sample for each sampling point). The mean results of the durability tests for the three sampling regions were visualized in bar plots.

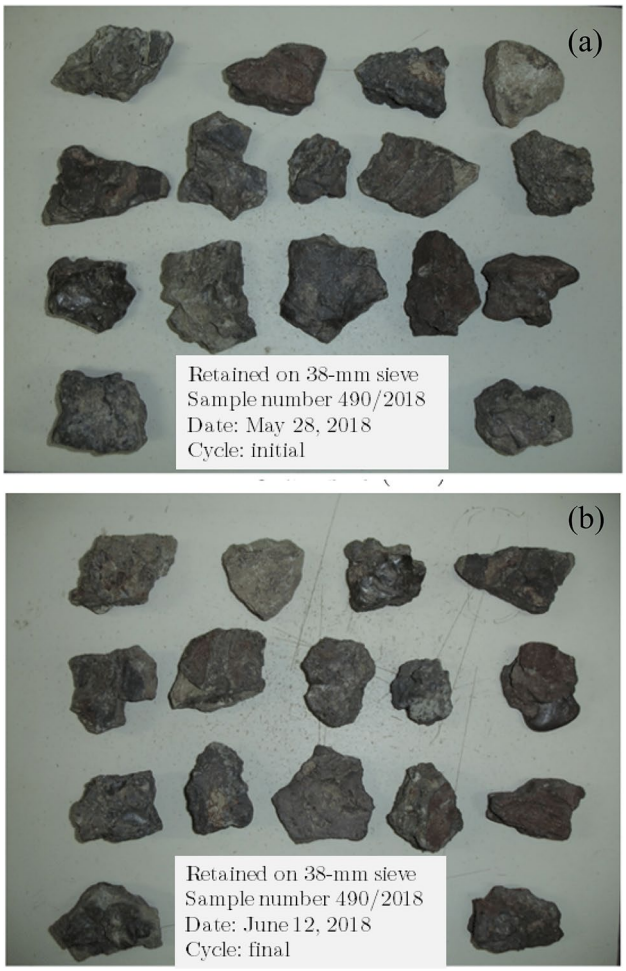

Fig. 3 FNS samples retained in a 38-mm sieve before (**a**) and after (**b**) accelerated cycling with ethylene glycol. The test was completed in 15 days

Chemical and mineralogical characterization

The chemical composition of the powdered byproduct was investigated using a wavelenght dispersive X-Ray Fluorescence (XRF) spectrometer. Mineralogical characterization using X-ray diffraction (XRD) analysis was performed with a Siemens D-5000 diffractometer, Cu $K\alpha_{1,2}$ radiation (λ =1.5408 Å), with voltage of 40 kV and amperage of 30 mA. These samples were step-scanned from 3 to 70° (2θ) in increments from 0.02° to 0.05° and time step of 1 s. The XRD patterns were analyzed with the help of the DiffracPlus EVA software (2009 version) using the International Centre for Diffraction Data (ICDD) database. Additionally, the shape, angularity, and surface texture of the FNS particles were analyzed using scanning electron microscopy (SEM). The VEGA3 Tescan SEM with variable vacuum (high and low), and double energy-dispersive X-ray spectroscopy (EDS) system from Oxford Instruments was used.

Design of granular rockfill dike

A free-draining rockfill dike is specifically designed to retain sediment, that is, to prevent water from transporting sediment downstream from the mining site where it was installed, thus reducing water turbidity. Dikes are installed in places that have a high rate of sediment generation and where environmental regulations restrict the release of sediments into water courses or existing ecosystems. Figure 4 displays the main features of a free-draining rockfill dike. Rockfill dikes differ from traditional embankment dams for multiple reasons [39]. Most notably, the structures are of small height (3–15 m), with a quite significant length. Moreover, the dikes are designed to carry discharge over their body (seepage). Because of these simpler characteristics, execution costs, surveillance and maintenance are usually minimal. The filter has the function of filtering water and retaining silts in the reservoir, consisting of sand (between 0.08 and 3.5 mm) with an average permeability of 10^{-4} m/s. The filter is designed based on well-known empirical criteria. To avoid abrupt changes between the silt and filter grain-size distributions, a transition layer is often designed. As illustrated by solid black bands in Fig. 4, transition layers may be placed to encapsulate the filter, which assists water filtration with a granulometric range between 4 and 19 mm and an average permeability of 10^{-3} m/s. Other transition materials can be placed between quarry rocks and rockfill, supporting the granulometric range transition. These transitions have a granulometric range between 75 and 250 mm and an average permeability of 10^{-2} m/s. After a period of time, silting may clog the void spaces in the coarser (rockfill) material [52], thereby favoring overtopping. Rockfill has the function of a permeable massif, helping in the water filtering process, and is thus constituted by aggregate in the granulometric range between 18 and 50 mm and with an average permeability of 10^{-3} m/s. Quarry rocks are used as a protection layer from extreme overflow to downstream (overtopping), preventing damage to the rockfill in eventual spills. These protection rocks are composed of aggregates in the granulometric range between 200 and 500 mm and with an average permeability of 10^{-2} m/s. In dry periods, it is then possible to clean the sediments naturally retained in the upstream face of the dike. In addition to regular maintenance of the dike, quick land rehabilitation of upland areas that provide notable amounts of eroded materials to the dike might avoid frequent dredging services.

In summary, the dike works like a large (byproduct) filter, sending cleaner water downstream. In this study, traditional criteria for filter design were adopted [53, 54]. Those criteria essentially consist of achieving two basic conditions. In the first condition, also known as retention criterion, the grain size of the filter should be small enough to retain the sediment. This criterion is defined as

$$\frac{D_{F(15)}}{D_{S(85)}} \leq 4 \text{ to } 5 \quad \text{(Condition 1)} \tag{1}$$

where $D_{F(15)}$ is the diameter through which 15% of filter material will pass and $D_{S(85)}$ represents the diameter through which 85% of sediment will pass. The second criterion, also referred to as permeability condition, suggests that the grain

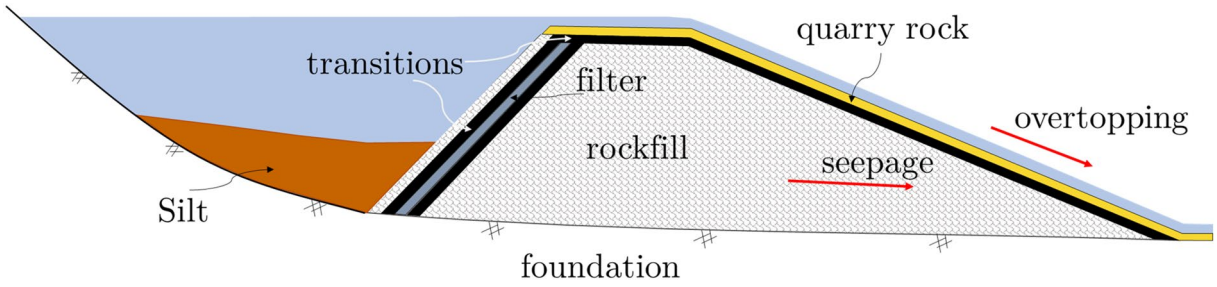

Fig. 4 Schematic overview of a free-draining rockfill dike. The structure is specifically designed to simultaneously contain sediment (retention criterion) and allow the rapid flow of water (permeability criterion). While the filter prevents migration of fine soil particles into the coarse (rockfill) material, water can flow through both seepage and overtopping

size of the filter should be large enough to enable a fast discharge of water, given as follows

$$\frac{D_{F(15)}}{D_{S(15)}} \geq 4 \text{ to } 5 \quad \text{(Condition 2)} \tag{2}$$

where $D_{S(15)}$ is the diameter through which 15% of sediment material will pass.

Results and discussion

Physical characterization

Figure 5a shows the particle size distribution curves of the 12 byproduct samples at locations 1 (light blue), 2 (medium blue) and 3 (sky blue). The results demonstrate that the particle size distributions of the investigated FNS are relatively similar, ranging from 0.01 to 37.50 mm. Sample S1-D (see Fig. 1) showed a higher presence of fines (24.3%) and sample S2-B exhibited greater gravel content (64.3%). The byproduct has predominantly higher contents of sand (29.5%) and gravel (53.4%), followed by silt (15.2%) and a low percentage of clay (1.9%). The mean particle size curves for each location are depicted in Fig. 5b and agree nicely with the mean curve for all samples, represented by the red line. Furthermore, the mean particle size curve is quite similar as those of other slag byproducts (e.g., [55, 56]). Table 3 summarizes the relevant granulometric indexes for each sampling location, including the grain-size diameters D_{10}, D_{30}, and D_{60}, the maximum particle size (D_{max}), the coefficients of uniformity (C_u) and curvature (C_c), and the fineness modulus (F_m). D_{max} values varied between 25 and 37.50 mm between all samples (with an average of 28.13 mm). The values of C_u, C_c, and F_m listed in Table 3 reflect a non-uniform (well graded) material and agree with values previously presented in the literature [8]. This result can be explained by the fact that the samples were not crushed and that no grain selection was executed prior to physical characterization.

Los Angeles test results are shown in Fig. 6 for each sampled location. The mean abrasion resistance below 30% is relatively low and fairly close to igneous rocks such as granites and Basalts (e.g., [57, 58]), likely due to the high contents of SiO_2 existing in FNS (see, e.g., [5, 17, 59]). A similar result was obtained by [60], who found a Los Angeles abrasion value of 25.8% for an alluvium aggregate of a rockfill dam located in China. Yet, since FNS is quickly air-cooled, its high content of amorphous and vitreous mineral [5] might significantly affect the abrasion resistance of the aggregate.

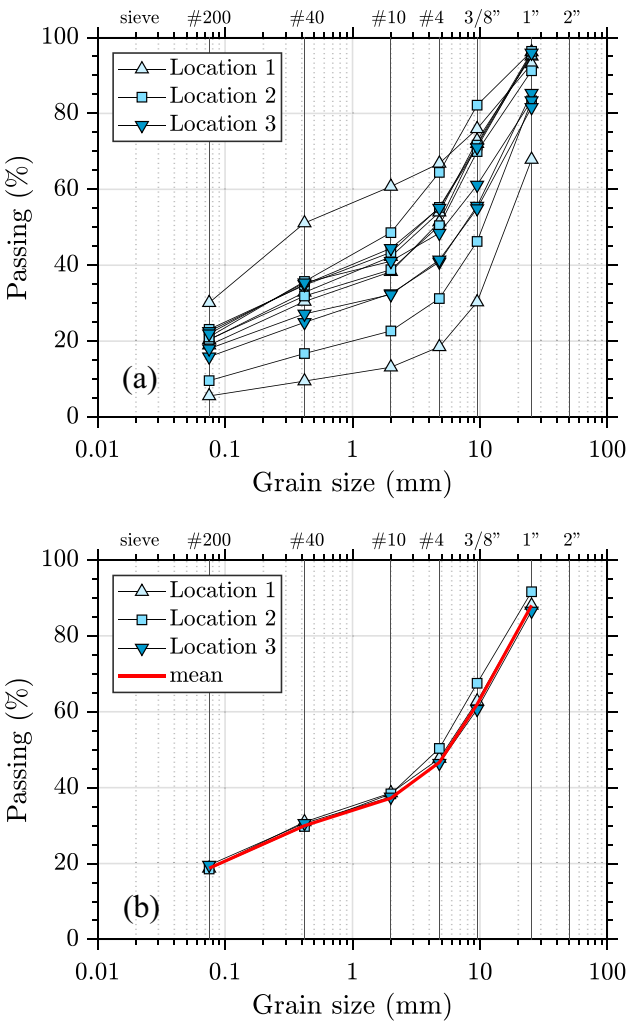

Fig. 5 Particle size distribution curves of the FNS samples. The top plot (**a**) highlights results obtained with 12 byproduct samples at locations 1 (light blue), 2 (medium blue) and 3 (sky blue). The bottom plot (**b**) shows results found for the mean particle size curves of each location. The solid red line in the bottom plot represents the mean grain-size curve for all byproduct samples

Leaching and dissolution tests

Tables 4 and 5 list summary data of the dissolution and leaching tests, respectively. From the reported data, it was observed that the average concentrations of the chemical elements appear unaffected by the sampling location. Moreover, these concentration values are lower than the maximum requirement of Brazilian standards [45, 46] as shown in the last columns of both tables. Exceptions are concentrations of iron and surfactants sampled at location 2 (Table 4). Thus, because of its iron and surfactants contents above the standard limits, the byproduct investigated is classified as Class II A (non-hazardous and non-inert). In Brazil, similar findings have been previously reported by [61], who observed concentrations of iron and phenols

Table 3 Summary of grain-size distribution and parameters of the FNS samples

Samples	Grain size (%)				D_{10}	D_{30}	D_{60}	D_{max}	C_u	C_c	F_m
	Gravel	Sand	Silt	Clay	(mm)	(mm)	(mm)	(mm)			
S1-A	58.5	25.8	14.1	1.7	0.032	0.40	5.6	25.0	175.0	0.9	4.02
S1-B	54.1	27.9	16.3	1.7	0.028	0.30	5.4	25.0	192.9	0.6	3.86
S1-C	63.2	26.5	9.5	0.8	0.600	6.00	10.3	37.5	17.2	5.8	5.33
S1-D	33.7	42.0	21.3	3.0	0.015	0.08	2.0	25.0	133.3	0.2	2.94
Mean	52.4	30.5	15.3	1.8	0.015	0.08	2.0	37.5	–	–	–
S2-A	53.2	28.0	16.9	1.9	0.021	0.20	5.4	25.0	257.1	0.4	3.76
S2-B	64.3	24.0	10.1	1.6	0.080	4.50	7.4	25.0	92.5	34.2	5.25
S2-C	55.0	29.5	14.9	0.6	0.026	0.30	6.7	37.5	257.7	0.5	4.08
S2-D	48.8	32.5	16.7	2.0	0.027	0.21	4.0	25.0	148.1	0.4	3.52
Mean	55.3	28.5	14.6	1.5	0.080	0.20	4.0	37.5	–	–	–
S3-A	53.0	27.3	15.8	4.0	0.018	0.20	5.5	25.0	305.6	0.4	3.78
S3-B	56.3	27.6	14.1	2.0	0.040	1.20	7.0	25.0	175.0	5.1	4.69
S3-C	46.3	34.0	19.0	0.7	0.032	0.16	6.2	25.0	193.8	0.1	4.13
S3-D	54.2	29.9	14.0	2.0	0.039	0.95	7.0	37.5	179.5	3.3	4.77
Mean	52.5	29.7	15.7	2.2	0.032	0.16	5.5	37.5	–	–	–

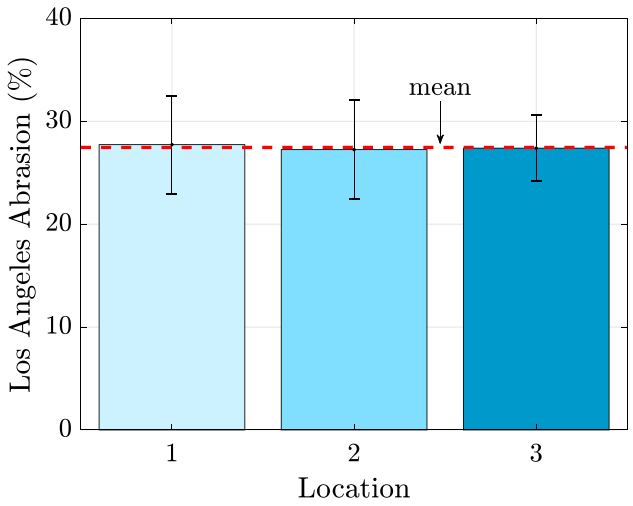

Fig. 6 Los Angeles abrasion test for each sampled location. The dashed red line indicates the mean value

Table 4 Summary of dissolution tests for FNS

Chemical elements	Average concentration (mg/L)			Upper limit (mg/L)
	Location 1	Location 2	Location 3	[48]
Aluminum	0.058	0.098	0.100	0.2
Arsenic	0.005	0.006	< 0.005	0.01
Barium	0.045	0.077	0.043	0.7
Cadmium	0.001	< 0.001	< 0.001	0.005
Lead	0.009	< 0.005	0.009	0.01
Cyanide	< 0.001	< 0.001	< 0.001	0.07
Chromium	< 0.003	< 0.003	< 0.003	0.05
Phenols	< 0.001	0.002	0.002	0.01
Fluoride	0.98	0.33	0.78	1.5
Mercury	< 0.0002	< 0.0002	< 0.002	0.001
Nitrate	0.075	0.850	0.175	10
Silver	0.002	0.008	0.007	0.05
Chloride	7.63	9.13	6.00	250
Copper	0.090	0.087	0.087	2
Iron	0.02	0.84	0.25	0.3
Manganese	0.008	0.067	0.016	0.1
Sodium	2.08	2.45	2.42	200
Surfactants	0.20	0.61	0.09	0.5
Sulfate	35.68	24.41	16.65	250
Zinc	< 0.02	< 0.02	< 0.02	5

of dissolved LD slag greater than the upper limit of the standard reference. However, as the byproduct must be crushed prior to dissolution tests according to the standard NBR 10006 [46], applications of FNS as coarse road aggregate and as rockfill dike material should not be an environmental concern. Dissolution tests for the classification of solid waste are performed on samples crushed in a range of less than 0.9 mm. However, the byproduct used in-situ is not crushed but is coarse instead, indicating that there is no elution problem. Furthermore, heavy metals like barium, cadmium, chromium, and lead showed relatively low leachability, with concentrations that were far below the permissible limit (Table 5). The findings thus agree with several others, which through leaching tests, reported that slag byproducts have a non-hazardous nature [62–64].

Table 5 Summary of leaching tests for FNS

Chemical elements	Average concentration (mg/L)			Upper limit (mg/L)
	Location 1	Location 2	Location 3	[48]
Barium	0.236	0.254	0.184	70
Cadmium	0.001	0.001	0.001	0.5
Chromium	0.755	0.536	0.527	5
Lead	0.009	0.009	0.010	1

Table 6 Mineralogical phases in FNS by XRD analyses

Group	Mineral	Chemical formula
Silicates	Akermanite	$Ca_2MgSi_2O_7$
	Albite	$NaAlSi_3O_8$
	Gismondine	$CaAl_2Si_2O_8 \cdot 4H_2O$
	Olivine	$(Mg, Fe)_2SiO_4$
	Quartz	SiO_2
Oxides	Ni/Cr Oxides	NiO, Cr_2O_3
	Hematite, Maghemite	Fe_2O_3
	Periclase	MgO
Sulfur phases	Fe/Ni Sulfate	$FeSO_4$, $NiSO_4(H_2O)_6$
	Sulfur	S
Clay minerals	Kaolinite	$Al_2Si_2O_5(OH)_4$
	Ilite	$3K_2O \cdot 11Al_2O_3 \cdot 26SiO_2 \cdot 8H_2O$
	Goethite	FeO(OH)

X-ray diffraction and fluorescence

Table 6 highlights the chemical characteristics of FNS used in this work obtained by X-ray diffraction (XRD) analyzes. Silicates comprise a major portion of the mineral fraction; oxides, clay minerals and sulfur phase are secondary groups. Kaolinite, illite and goethite were observed only in three of the twelve sampling points in Fig. 1. This finding is consistent with our weathering test data, which demonstrate relatively low changes in mass after cycling, indicating the absence of potential expansive minerals (to be supported here later by cycling tests).

The main chemical components of FNS obtained by XRF tests are outlined in Table 7. The percentages listed summarize the mean values of the chemical compounds for each sampling location. XRF tests performed at all locations of the stockpile indicated quite similar chemical compositions, predominantly with silica (SiO_2)—49.07%, magnesium oxide (MgO)—29.05% and ferric oxide (Fe_2O_3)—15.57%. Several observed similar chemical compositions of the FNS [8, 9, 19, 20, 65]. However, the MgO and CaO contents differ substantially from previous studies [10, 27], arguably due to the distinct origins of raw materials and smelting techniques during the extraction of ferronickel alloys [7]. The high MgO content might influence the expansive behavior of the byproduct. The occurrence of free periclase MgO in FNS samples demonstrates a potential for expansive hydration reactions [38]. Although the expansion potential is not a particular problem to be considered in the case of the proposed free-draining dike, one should be particularly careful, however, not to use this byproduct for the application in pavement layers since its use enhances the chances of expansion. Yet, the FNS described here might be successfully applied as a road material using blended soil-byproduct mixtures [28, 56]. This investigation is a current ongoing research project at the Federal University of Ouro Preto.

Table 7 Chemical composition (%) of FNS by XRF tests

	Location 1	Location 2	Location 3
MgO	29.42	29.01	28.73
Al_2O_3	2.39	2.64	2.75
SiO_2	49.26	48.76	49.18
CaO	0.62	0.53	0.43
MnO	0.34	0.36	0.27
Fe_2O_3	15.27	26.0	15.34
SO_3	0.07	0.05	0.12
Other	4.4	1.3	3.18

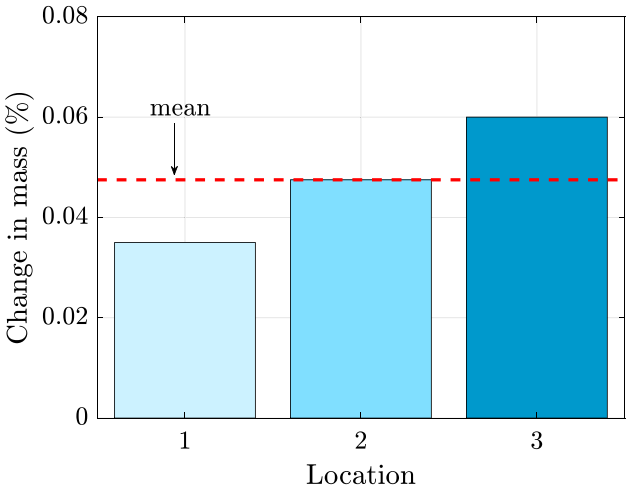

Fig. 7 Results of ethylene glycol accelerated weathering test

Cycling

Accelerated weathering cycling tests with ethylene glycol (Fig. 7) demonstrate that the byproduct does not undergo premature disaggregation in the presence of water for all sampled locations. The results show a mean change in mass of 0.05%, thereby indicating no evidence of cracking, disintegration, or chipping. For instance, informal visual

inspection of FNS samples (Fig. 3) suggests that the shape of the byproduct is hardly changed after cycling tests. This is an important finding in that it reflects the lack of expansive minerals in the FNS. Furthermore, the low levels of CaO identified in the XRF and XRD tests, nicely agree with the cycling test results. Indeed, excessive free lime content is considered the primary culprit that can lead to premature expansion and disintegration of slag byproducts and, consequently, loss of strength [66, 67]. Here, the accelerated weathering cycling tests showed no particle size reduction and therefore no fine particle generation. As a result, this leads to a reduction in clogging probability, inspiring confidence in our proposal to use FNS as a free-draining rockfill dike. Yet, mechanical properties of the dike material, such as hydraulic conductivity and piping resistance are not discussed in this paper, and thus more focused studies of these mechanical properties of FNS may be worthwhile.

Scanning electron microscopy

SEM images of representative FNS samples have indicated regions with two distinct microstructures (Fig. 8). The first region has a massive matrix (a) with micropores between non-crystallized phases and few empty embedded air pores (spherical aspect in Fig. 8b), morphologies that agree with previous investigations (e.g., [9, 17]). Such voids are likely formed during the cooling of the slag. The second region has a macroporous matrix with a variety of poorly (c) to very well crystallized phases (d). These well crystallized phases include minerals such as olivine, pyroxene and feldspar. Air pores do not have a homogeneous pattern. Parts of the samples have a high concentration of air pores, while other parts are massive and exhibit only dispersed air pores. Rare phase agglomerations, such as aragonite ($CaCO_3$) and iron oxyhydroxides, with dimensions of 5 μm, were also observed in pores. Some samples had a cemented crust with rare micropores, composed of a higher concentration of the chemical elements iron (Fe), chromium (Cr) and manganese (Mn). This pattern is illustrated in Fig. 9, with a detailed SEM image of a Fe-concentrated crust.

Ferronickel slag granular filter

FNS thus far have demonstrated excellent durability performance and favorable environmental characteristics, a fact that encouraged us to design its reuse as a granular rockfill dike. To give a better understanding of the practical nature of the present paper, we next illustrate in Fig. 10, the grain-size distribution of the different components of a rockfill dike (top) and their corresponding zones in a conceptual cross section. These include the body of the dike (rockfill), a sand filter, quarry rock at the dam crest, two transition layers, and the sediment to be retained. In this work, FNS is indicated for rockfill and transition layers. To simplify the graphical interpretation, the colors of each particle size range in the top panel display the same color scale as those of the dike (bottom panel). Based on the grain-size curves of the sediment, grain-size curves of suitable filter material were proposed using the empirical relations of Eqs. 1 and 2. For example, consider the lower bound of the sediment particle size distribution. Then, from Fig. 10, $D_{S(15)}$ and $D_{S(85)}$ are 0.001 and 0.011 mm, respectively. Accordingly, considering the lower bound of the filter (sand) particle size distribution, $D_{F(15)}$ is 0.15 mm. Thus, the value of $D_{F(15)}/D_{S(85)}$ is 1.36 (Eq. 1) and $D_{F(15)}/D_{S(15)}$ is 150 (Eq. 2), which satisfy conditions 1 (retention) and 2 (permeability) of the traditional criteria adopted herein. The same exercise is also performed for the upper bounds of the particle size distributions. Once the particle size distribution of the filter is defined, the transitions, rockfill, and quarry rock layers are estimated in a similar way.

The grain-size characteristics of the investigated byproduct enable its use not only as a rockfill but also as transition materials. Note that if the grain size of the sediment changes, the design of the dike needs to be reassessed. As outlined in Fig. 10 (bottom), the proposed cross section illustrates that a considerable amount of FNS could be used for the construction of dikes. Yet, as the particle size distribution curves of the investigated samples (Fig. 5a) were found to vary, care should be exercised to select the appropriate material. Indeed, FNS samples evaluated in Fig. 5 were obtained directly from the company's stockpile, that is, they did not undergo any granulometric selection. Therefore, an in-situ soil separation plant should be an effective way to properly adjust the FNS granulometric ranges. A smaller amount of other natural materials could be used to compose the filter (sand) and the dike crest (quarry rock), since much effort would be required to adjust the FNS granulometry to those of the filter and quarry rock. As a consequence, FNS, an environmentally friendly and cost-free material, could make mining and metallurgical companies far more sustainable.

Figure 10 proposes a cross section with different materials for the filter, transitions, and crest of the dike. The rockfill dike could be built with FNS without grain-size separation. This would reduce the construction costs at the expense of increased maintenance costs. The probability of clogging would arguably be higher, since the absence of a filter would facilitate the clogging of the dike's interior, thus increasing maintenance costs. In contrast, the use of a filter and transition layers will not prevent possible clogging, but it would facilitate filter replacement, thus reducing maintenance costs. In summary, granulometric separation of the FNS stockpiled is a condition of the rockfill dike design, as proposed in Fig. 10. More studies and monitoring are needed to establish whether the proposed free-draining rockfill dike will provide a satisfactory operational life.

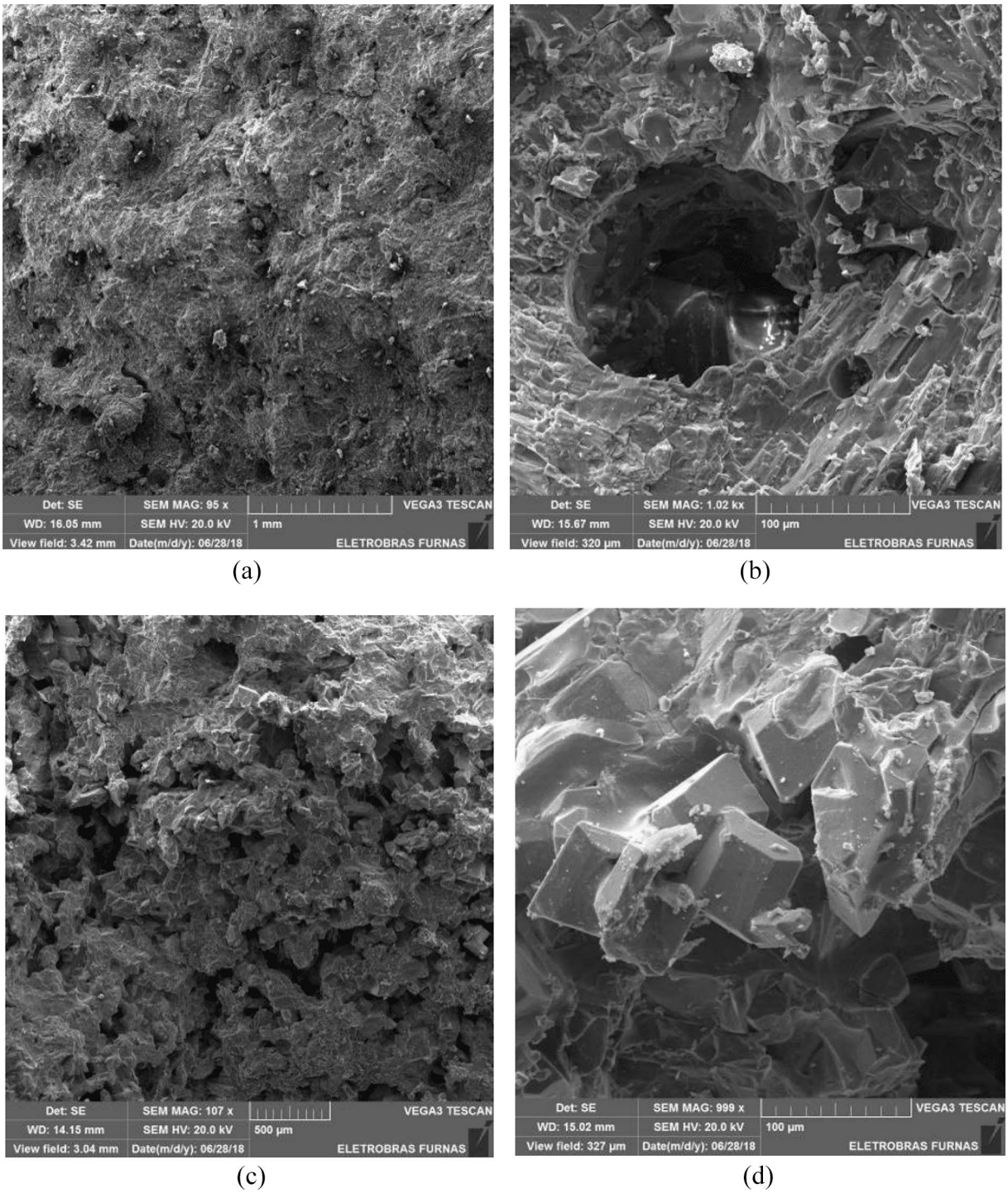

Fig. 8 SEM images of FNS: **a** massive region, **b** embedded air pore, **c** macroporous region with poorly formed to very well crystallized phases, and **d** detail of well crystallized phases

It is estimated that about 50,000 m^3 of byproduct could be used in the construction of a dike in a nearby watershed, representing a 2.77% reduction in the current volume stockpiled. However, the company's large industrial area allows the construction of up to 25 dykes, which can reduce the current volume of the byproduct stocked by approximately 70%. This illustrates the potential contribution of the FNS to the promotion of sustainability in mining sites. Furthermore, the reuse of this byproduct within mined areas reduces greenhouse gas emissions related to transportation,

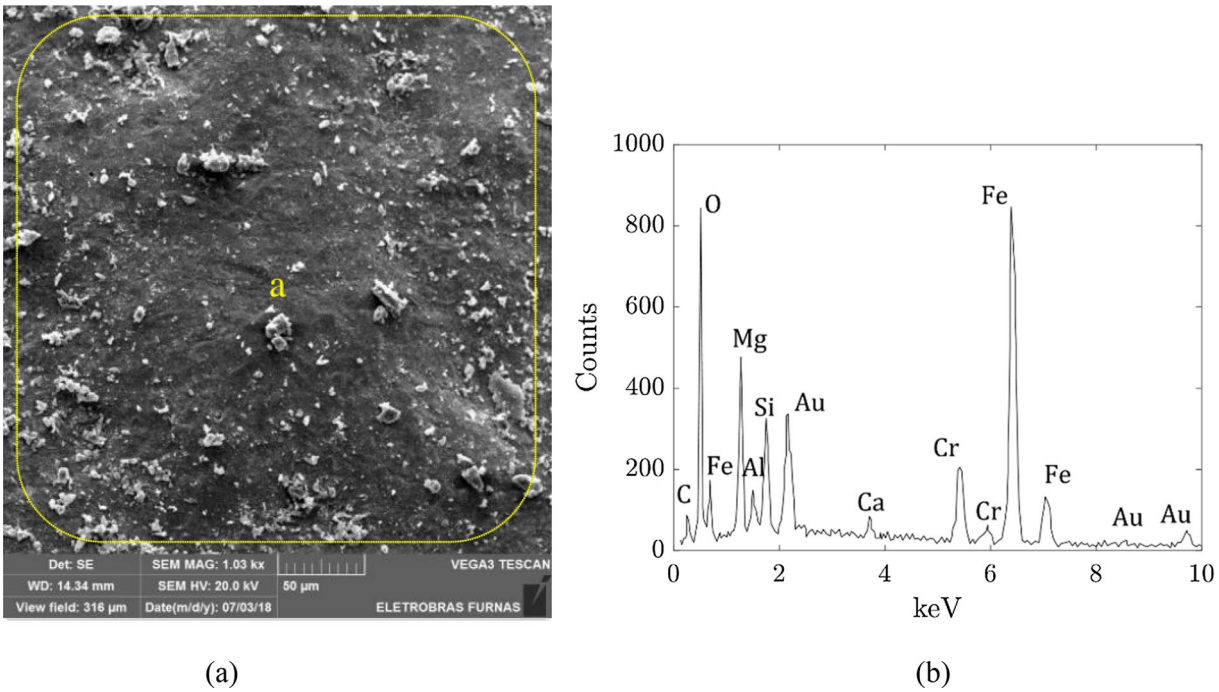

Fig. 9 SEM image of Fe-concentrated crust (**a**) and its respective EDS spectrum (**b**)

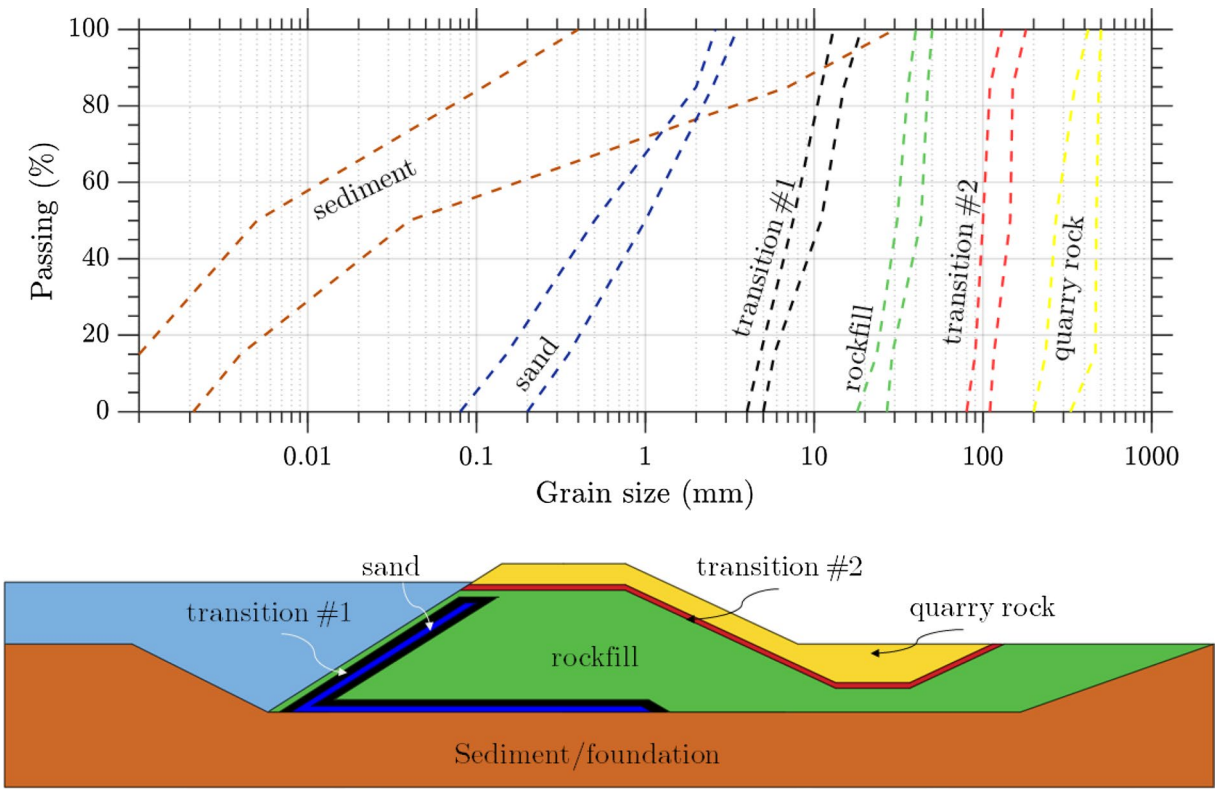

Fig. 10 Grain size curves (top plot) of the dike's different features, including the sediment to be retained, suitable filter materials, rockfill and quarry rock. In the bottom panel, a schematic free-draining FNS rockfill dike is proposed (not to scale)

thus enabling a cleaner production in the mining and metals sector. Interestingly, during the maintenance of the dike, another sustainable measure can still be implemented. Sediments retained in the upstream face of the rockfill dike, and the deteriorated filter and transitions can be reused by removing the fine silt, for example, through an in-situ soil separation plant. As the silt from the site tends to be rich in nickel and iron, this material can be reused in the iron-nickel alloy enrichment process. While the costs of implementing an FNS separation structure are not high for global companies, smaller companies must evaluate the construction of the separation plant in a multi-objective approach, considering technical, economic, and environmental trade-offs.

Comparison with natural aggregate rockfill materials

To provide more insights on the characteristics of rockfill dike materials, consider Table 8, which lists the physical properties of samples from different studies [68–70]. These data include engineering properties of granite, gneiss and basalt used in rockfill dams, and allow us to compare the properties of the investigated byproduct (last column) against other common crystalline rocks from Brazil. The high C_u-value of the byproduct reflects the non-uniform nature of its particles. Similarly to natural aggregates selected in quarries, a careful separation of grain size must be carried out before using the byproduct. One should notice that the diameter values of the listed natural rocks used in rockfill dams are greater than the maximum diameter of the byproduct. If a larger size material is required for a free-draining rockfill dike (e.g., protection under overtopping conditions), then it is convenient to use quarry rock (Fig. 10). The higher specific gravity of the FNS is attributed to its high iron oxide content [38]. Although Los Angeles abrasion is a measure that varies greatly depending on the mineralogical characteristics of geomaterials, the behavior of FNS was similar to that of natural aggregates. The same holds true for water absorption, change in mass and UCS values, which makes the material suitable to be used as a rockfill dike. Similar results were obtained by [67], who found that basic oxygen furnace slag aggregates exhibit superior physical and mechanical characteristics compared to most natural rocks.

Conclusions

This study investigated the feasibility of using ferronickel slag as free-draining rockfill dike materials for mining sediment control. Sediment control and waste management have long been a challenge in nickel producing regions. The use of FNS in dikes, with an adequate granulometric selection, compatible with the grain size of the silts, represents a promising waste solution for the ferronickel sector and the value chains of stainless steel and other derived products. Based on a series of laboratory tests involving physical, environmental, material durability, chemical and mineralogical characterization, the following conclusions were drawn:

- Physical characterization revealed that particle sizes of the FNS are distributed over a wide range, requiring grain-size separation before use. Based on these granulometric characteristics, the material was considered suitable as rockfill and transition layers in free-draining dikes. The mean abrasion resistance below 30% is relatively low and similar to aggregates used in rockfill dams.
- Laboratory investigations did not indicate environmental problems. Indeed, the average concentrations of chemical elements after leaching and solubilization tests were below standard requirements. This is an important finding since the non-hazardous FNS would work as a water filter, partially submerged depending on rainfall.
- Accelerated weathering cycling tests with ethylene glycol revealed excellent durability, since no expansive minerals

Table 8 Engineering properties of different rocks used as (natural) rockfill materials

Property	Basalt[a]	Gneiss[b]	Granite[b]	Weathered basalt[c]	Basalt[c]	This work
C_u	5.1	n.a.[d]	n.a	1.12	1.12	177.3
C_c	n.a	n.a	n.a	2.7	2.7	4.3
D_{max}(mm)	76	25–150	25–200	152	152	28
Los Angeles (%)	n.a	57–63	22	n.a	n.a	27
Specific gravity	2.8	2.5	2.6	1.8	1.8	3.3
Water abs. (%)	0.5	0.4–11	0.4	n.a	n.a	1.2
UCS (MPa)	292	47–57	160–180	238	180	139
Change in mass (%)	n.a	0.03	n.a	n.a	n.a	0.05

The values reported in the literature include data from basalt, granite and gneiss. The last column lists properties of FNS, the byproduct investigated in this work

[a][68], [b][69], [c][67], [d]Not available

were identified that could indicate premature disaggregation of FNS in the presence of water.

- XRD analyzes indicated that FNS is mostly composed by silicates, and oxides and sulfur phase are secondary mineral groups. XRF tests revealed that SiO_2 (49.07%), MgO (29.05%) and Fe_2O_3 (15.57%) are the main chemical components of the byproduct. SEM images confirmed these findings and demonstrated the massive and crystallized nature of the byproduct, with embedded air pores.
- FNS has different grain-size ranges, small enough to prevent the transport of sediments through the dike and sufficiently large to offer drainage, thereby enabling its (re)use as a free-draining granular rockfill dike, reducing its current volume stockpiled.
- The proposed waste solution for mining regions should honor, however, technical, economic, and environmental trade-offs, as reuse of FNS requires construction and operational costs.

Acknowledgements The authors greatly acknowledge financial support from the Brazilian National Council for Scientific and Technological Development, CNPq. We wish to thank DF+ Engineering and Geominas for the help with laboratory and field work. The quality of this paper has been greatly enhanced by the constructive comments of two anonymous reviewers and editors handling this manuscript.

Author contributions JPRC: Conceptualization, Methodology, Formal analysis, Investigation, Data curation, Writing—original draft preparation. GJCG: Formal analysis, Validation, Writing—original draft preparation, Writing—review and editing. GF: Supervision, Investigation, Resources. DMM: Investigation, Visualization. AF: Formal analysis, Writing—review and editing. PJMP: Formal analysis, Validation.

Declarations

Conflict of interest On behalf of all authors, the corresponding author states that there is no conflict of interest.

References

1. Fitzpatrick P, Fonseca A, McAllister ML (2011) From the Whitehorse mining initiative towards sustainable mining: lessons learned. J Clean Prod 19(4):376–384. https://doi.org/10.1016/j.jclepro.2010.10.013
2. Tost M, Hitch M, Chandurkar V, Moser P, Feiel S (2018) The state of environmental sustainability considerations in mining. J Clean Prod 182:969–977. https://doi.org/10.1016/j.jclepro.2018.02.051
3. Polyakov O (2013) Technology of ferronickel. In: Gasik M (ed) Handbook of ferroalloys. Butterworth-Heinemann, Oxford, pp 367–375. https://doi.org/10.1016/C2011-0-04204-7
4. Crundwell F, Moats M, Ramachandran V, Robinson T, Davenport W (2011) Smelting of laterite ores to ferronickel. Extractive metallurgy of nickel, cobalt and platinum group metals. Elsevier, Oxford, pp 67–83. https://doi.org/10.1016/C2009-0-63541-8
5. Huang Y, Wang Q, Shi M (2017) Characteristics and reactivity of ferronickel slag powder. Constr Build Mater 156:773–789. https://doi.org/10.1016/j.conbuildmat.2017.09.038
6. Saha AK, Khan M, Sarker PK (2018) Value added utilization of byproduct electric furnace ferronickel slag as construction materials: a review. Resour, Conserv Recycl 134:10–24. https://doi.org/10.1016/j.resconrec.2018.02.034
7. Choi YC, Choi S (2015) Alkali–silica reactivity of cementitious materials using ferro-nickel slag fine aggregates produced in different cooling conditions. Constr Build Mater 99:279–287. https://doi.org/10.1016/j.conbuildmat.2015.09.039
8. Saha AK, Sarker PK (2016) Expansion due to alkali-silica reaction of ferronickel slag fine aggregate in OPC and blended cement mortars. Constr Build Mater 123:135–142. https://doi.org/10.1016/j.conbuildmat.2016.06.144
9. Long W-J, Peng J-K, Gu Y-C, Li J-L, Dong B, Xing F, Fang Y (2021) Recycled use of municipal solid waste incinerator fly ash and ferronickel slag for eco-friendly mortar through geopolymer technology. J Clean Prod 307:127281. https://doi.org/10.1016/j.jclepro.2021.127281
10. Bao J, Yu Z, Wang L, Zhang P, Wan X, Gao S, Zhao T (2021) Application of ferronickel slag as fine aggregate in recycled aggregate concrete and the effects on transport properties. J Clean Prod 304:127149. https://doi.org/10.1016/j.jclepro.2021.127149
11. Luo Z, Ma Y, Mu W, Liu J, He J, Zhou X (2021) Magnesium phosphate cement prepared with electric furnace ferronickel slag: properties and its hydration mechanism. Constr Build Mater 300:123991. https://doi.org/10.1016/j.conbuildmat.2021.123991
12. Xi B, Li R, Zhao X, Dang Q, Zhang D, Tan W (2018) Constraints and opportunities for the recycling of growing ferronickel slag in China. Resour, Conserv Recycl 139:15–16. https://doi.org/10.1016/j.resconrec.2018.08.002
13. Kuri JC, Khan MNN, Sarker PK (2021) Fresh and hardened properties of geopolymer binder using ground high magnesium ferronickel slag with fly ash. Constr Build Mater 272:121877. https://doi.org/10.1016/j.conbuildmat.2020.121877
14. Yang T, Wu Q, Zhu H, Zhang Z (2017) Geopolymer with improved thermal stability by incorporating high-magnesium nickel slag. Constr Build Mater 155:475–484. https://doi.org/10.1016/j.conbuildmat.2017.08.081
15. Nguyen QD, Khan MSH, Castel A, Kim T (2019) Durability and microstructure properties of low-carbon concrete incorporating ferronickel slag sand and fly ash. J Mater Civil Eng. https://doi.org/10.1061/(ASCE)MT.1943-5533.0002797
16. USGS (2022) Mineral commodity summaries. Tech. rep., U.S. Geological Survey (2022). https://doi.org/10.3133/mcs2022
17. Sun J, Feng J, Chen Z (2019) Effect of ferronickel slag as fine aggregate on properties of concrete. Constr Build Mater 206:201–209. https://doi.org/10.1016/j.conbuildmat.2019.01.187
18. Cosme J, Fernandes G, Fernandes DP (2021) Utilization of ferronickel slag in hot mix asphalt. REM - Int Eng J 74(1):19–26. https://doi.org/10.1590/0370-44672019740068
19. Kallas FPE (2015) Valorization of the slag generated in the production of nickel as a raw material for the production of ceramic tiles, Master thesis, University of Ribeirão Preto, São Paulo, Brazil, in Portuguese
20. Silva MM, Safatle FA, Pereira HS, Oliveira KD, Avila-Neto CN (2017) Recovery of the slag from the nickel ore reduction furnace for use as a fertilizer. In: Blucher chemical engineering proceedings, pp. 2813–2818. https://doi.org/10.5151/chemeng-cobeq ic2017-448 (in Portuguese)
21. Kim Y, Kim M, Sohn J, Park H (2018) Applicability of gold tailings, waste limestone, red mud, and ferronickel slag for producing glass fibers. J Clean Prod 203:957–965. https://doi.org/10.1016/j.jclepro.2018.08.230
22. Shang W, Peng Z, Huang Y, Gu F, Zhang J, Tang H, Yang L, Tian W, Rao M, Li G, Jiang T (2021) Production of glass-ceramics from metallurgical slags. J Clean Prod 317:128220. https://doi.org/10.1016/j.jclepro.2021.128220

23. Zulhan Z, Agustina N (2021) A novel utilization of ferronickel slag as a source of magnesium metal and ferroalloy production. J Clean Prod 292:125307. https://doi.org/10.1016/j.jclepro.2020.125307
24. Saha AK, Sarker PK (2017) Sustainable use of ferronickel slag fine aggregate and fly ash in structural concrete: mechanical properties and leaching study. J Clean Prod 162:438–448. https://doi.org/10.1016/j.jclepro.2017.06.035
25. Naruzzuman M, Camargo Casimiro JO, Sarker PK (2020) Fresh and hardened properties of high strength self-compacting concrete using byproduct ferronickel slag fine aggregate. J Build Eng 32:101686. https://doi.org/10.1016/j.jobe.2020.101686
26. Rahman MA, Sarker PK, Shaikh FUA, Saha AK (2017) Soundness and compressive strength of Portland cement blended with ground granulated ferronickel slag. Constr Build Mater 140(554):194–202. https://doi.org/10.1016/j.conbuildmat.2017.02.023
27. Lemonis M, Tsakiridis P, Katsiotis N, Antiohos S, Papageorgiou D, Katsiotis M, Beazi-Katsioti M (2015) Hydration study of ternary blended cements containing ferronickel slag and natural pozzolan. Constr Build Mater 81:130–139. https://doi.org/10.1016/j.conbuildmat.2015.02.046
28. Gomes GJC, Magalhães AJ, Rocha FLL, Fonseca A (2021) A sustainability-oriented framework for the application of industrial byproducts to the base layers of low-volume roads. J Clean Prod 295:126440. https://doi.org/10.1016/j.jclepro.2021.12644
29. Graedel T, Allenby B (eds) (2009) Industrial ecology and sustainable engineering. Prentice Hall, New York
30. Hester RE, Hrrison RM (eds) (1994) Mining and its environmental impact, 1st edn. The Royal Society of Chemistry, Cambridge
31. Wantzen KM, Mol JH (2013) Soil erosion from agriculture and mining: a threat to tropical stream ecosystems. Agriculture 3:660–683. https://doi.org/10.3390/agriculture3040660
32. Jaramilo F, Bacard M, Narinesingh P, Gaskin S, Cooper V (2016) Assessing the role of a limestone quarry as sediment source in a developing tropical catchment. Land Degrad Dev 27(4):1064–1074. https://doi.org/10.1002/ldr.2347
33. Zapico I, Laronne JB, Meixide C, Sánchez Castillo L, Martín Duque JF (2021) Evaluation of sedimentation pond performance for a cleaner water production from an open pit mine at the edge of the alto Tajo natural park. J Clean Prod 280:124408. https://doi.org/10.1016/j.jclepro.2020.124408
34. Gupta AK (2016) Effects of particle size and confining pressure on breakage factor of rockfill materials using medium triaxial test. J Rock Mech Geotech Eng 8(1):378–388. https://doi.org/10.1016/j.jrmge.2015.12.005
35. Zhai Y, Li L, Chapuis RP (2021) Analytical, numerical and experimental studies on steady-state seepage through 3D rockfill trapezoidal dikes. Mine Water Environ 40:931–942. https://doi.org/10.1007/s10230-021-00798-8
36. Escavy J, Herrero M, Lopez-Acevedo F, Trigos L (2022) The progressive distancing of aggregate quarries from the demand areas: magnitude, causes, and impact on CO_2 emissions in Madrid region (1995–2018). Res Policy 75:102506. https://doi.org/10.1016/j.resourpol.2021.102506
37. Brito A, Caldeira LMMS, Maranha JR (2018) Hydromechanical characterization of soil-rockfill mixtures. J Mater Civil Eng 30(7):04018123. https://doi.org/10.1061/(ASCE)MT.1943-5533.0002295
38. Yildirim IZ, Prezzi M (2015) Geotechnical properties of fresh and aged basic oxygen furnace steel slag. J Mater Civil Eng 27(12):04015046. https://doi.org/10.1061/(ASCE)MT.1943-5533.0001310
39. Novak P, Moffat A, Nalluri C, Narayanan R (2007) Hydraulic structures, 4th edn. SCRC, London. https://doi.org/10.1201/9781315274898
40. Siddiqua S, Blatz J, Privat N (2013) Evaluating the behaviour of instrumented prototype rockfill dams. Can Geotech J 50(3):298–310. https://doi.org/10.1139/cgj-2011-0371
41. Varadarjan A, Sharma KG, Venkatachalam K, Gupta AK (2003) Testing and modeling two rockfill materials. J Geotech Geoenviron Eng 129(3):206–218. https://doi.org/10.1061/(ASCE)1090-0241(2003)129:3(206)
42. ABNT (2011) Railway - Ballast - Requirements and test methods. ABNT NBR 5564. Rio de Janeiro, Brazil: Brazilian Association of Technical Standards
43. ABNT (2016) Soil – granulometric analysis. ABNT NBR 7181. Rio de Janeiro, Brazil: Brazilian Association of Technical Standards
44. ABNT (2001) Small-size coarse aggregate - test method for resistance to degradation by Los Angeles machine. ABNT NBR NM 51. Rio de Janeiro, Brazil: Brazilian Association of Technical Standards
45. ABNT (2004) Procedure for obtention leaching extract of solid wastes. ABNT NBR 10005. Rio de Janeiro, Brazil: Brazilian Association of Technical Standards
46. ABNT (2004) Procedure for obtention of solubilized extraction of solid wastes. ABNT NBR 10006. Rio de Janeiro, Brazil: Brazilian Association of Technical Standards
47. ABNT (1992) Aggregates - soundness by immersion in ethyleneglycol - method of test. ABNT NBR 12697. Rio de Janeiro, Brazil: Brazilian Association of Technical Standards.
48. USEPA (1992) Method - Toxicity characteristics leaching procedure (TCLP), EPA SW846, U.S. Environmental Protection Agency
49. ABNT (2004) Solid waste - classification. Rio de Janeiro, ABNT NBR 10004. Brazil: Brazilian Association of Technical Standards
50. van Blerk PGL, Fletcher E, Costello SB, Henning TFP (2017) Ethyleneglycol accelerated weathering test: an improved, objective aggregate durability test method. Transp Res Rec 2655(1):27–35. https://doi.org/10.3141/2655-05
51. Leyland RC, Paige-Green P, Momayez M (2014) Development of the road aggregate test specifications for the modified ethylene glycol durability index for basic crystalline materials. J Mater Civil Eng 26(7):04014028. https://doi.org/10.1061/(ASCE)MT.1943-5533.0000946
52. Das BM, Sobhan K (2017) Principles of geotechnical engineering, 9th edn. Cengage Learning, Massachusetts
53. Terzaghi K, Peck RB (eds) (1948) Soil mechanics in engineering practice, 1st edn. Wiley, New York
54. Mitchell R (ed) (1983) Earth structures engineering, 1st edn. Allen & Unwin, Winchester, MA
55. Cikmit AA, Tsuchida T, Hashimoto R, Honda H, Kang G, Sogawa K (2019) Expansion characteristic of steel slag mixed with soft clay. Constr Build Mater 227:116799. https://doi.org/10.1016/j.conbuildmat.2019.116799
56. Magalhães AJ, Gomes GJC, Pires PJM (2020) Toward improved performance of unpaved roads: laboratory tests and field investigation of a soil-byproduct base layer. Road Mater Pavement Des 23(1):184–198. https://doi.org/10.1080/14680629.2020.1809503
57. Kılıç A, Atis C, Teymen A, Karahan O, Ozcan C, Bilim C, Ozdemir M (2008) The influence of aggregate type on the strength and abrasion resistance of high strength concrete. Cement Concrete Compos 30(4):290–296. https://doi.org/10.1016/j.cemconcomp.2007.05.011
58. Teymen A (2019) Estimation of Los Angeles abrasion resistance of igneous rocks from mechanical aggregate properties. Bull Eng Geol Environ 78:837–846. https://doi.org/10.1007/s10064-017-1134-0
59. Adomako S, Engenlsen CJ, Thorstensen RT, Barbieri DM (2021) Review of the relationship between aggregates geology and Los

Angeles and micro-Deval tests. Bull Eng Geol Environ 80:1963–1980. https://doi.org/10.1007/s10064-020-02097-y
60. Xiao Y, Liu H, Chen Y, Jiang J (2014) Strength and deformation of rockfill material based on large-scale triaxial compression tests. i: Influences of density and pressure. J Geotech Geoenviron Eng 140(12):04014070. https://doi.org/10.1061/(ASCE)GT.1943-5606.0001176
61. Bastos LAC, Silva GC, Mendes JC, Peixoto RAF (2016) Using iron ore tailings from tailing dams as road material. J Mater Civil Eng 28(10):04016102. https://doi.org/10.1061/(ASCE)MT.1943-5533.0001613
62. Tossavainen M, Forssberg E (1999) The potential leachability from natural road construction materials. Sci Total Environ 239(1):31–47. https://doi.org/10.1016/S0048-9697(99)00283-1
63. Barisic I, Grubesa IN, Kutuzovic BH (2017) Multidisciplinary approach to the environmental impact of steel slag reused in road construction. Road Mater Pavement Design 18(4):897–912. https://doi.org/10.1080/14680629.2016.1197143
64. Chand S, Paul B, Kumar M (2017) Short-term leaching study of heavy metals from LD slag of important steel industries in Eastern India. J Mater Cycles Waste Manag 19:851–862. https://doi.org/10.1007/s10163-016-0486-z
65. Cao R, Jia Z, Zhang Z, Zhang Y, Banthia N (2020) Leaching kinetics and reactivity evaluation of ferronickel slag in alkaline conditions. Cement Concrete Res 137:106202. https://doi.org/10.1016/j.cemconres.2020.106202
66. Coomarasamy A, Walzak TL (1995) Cost–benefit analysis of RAP–sand blend applications in road construction. Transp Res Rec 1492:85–95
67. Kambole C, Paige-Green P, Kupolati W, Ndambuki J, Adeboje A (2017) Basic oxygen furnace slag for road pavements: a review of material characteristics and performance for effective utilization in southern Africa. Constr Build Mater 148:618–631. https://doi.org/10.1016/j.conbuildmat.2017.05.036
68. Maia PCA (2001) Evaluation of geomechanical and alterability behaviour of rockfills, Master thesis, Pontifical Catholic University of Rio de Janeiro, Rio de Janeiro, Brazil, in Portuguese
69. Basso VR (2007) Stress-strain study for one rockfill aiming concrete face rockfill dam, Master's thesis, University of São Paulo, São Paulo, Brazil, in Portuguese
70. Santos ACC (2019) Critical analysis of the forecasting of mechanical behavior of rockfill by laboratory scale modeling, Phd thesis, University of Brasília, Brasília, Brazil, in Portuguese